

Analytical Representation of Stroboscopic Maps of Ordinary Nonlinear Differential Equations

W. Eberl, M. Kuchler, A. Hübler*, and E. Lüscher

Physik Department, Technische Universität München, Garching,
 Federal Republic of Germany

M. Maurer and P. Meinke

MAN Technologie, München, Federal Republic of Germany

Received May 5, 1987

Dedicated to Professor Harry Thomas on the occasion of his 60th birthday

The stroboscopic map of some nonlinear dynamical systems can be described by means of a series expansion with only few non-trivial coefficients, provided that the frequency of the stroboscope coincides with the basic frequency of the oscillator. An analytic representation of such a 'simple' map can be obtained by the following two methods: (i) analytical integration of the ordinary differential equation, or (ii) numerical integration on a discrete grid scheme and subsequent approximation by an appropriate series of functions.

1. Introduction

Oscillators with marked nonlinearity and chaotic solutions represent good mathematical models in various fields of physics, as in classical mechanics [1], electrodynamics [2, 3], medical techniques [4], physical chemistry [5], geophysics [6], etc. Also problems of the classical field theory can often be traced back to those differential equations [7–9]. In general these differential equations are not integrable [10], and, they cannot be traced back to known basic functions, although their dynamics can be numerically simulated. Nevertheless it was shown that essential properties of the dynamics can be described by iteration functions (Poincaré-map, stroboscopic map) [11, 12]. These iteration functions can be much simpler [13] than the original differential equation. They can easily be solved numerically and are mathematically well examined [14–17]. Iteration functions were at first

used in physics by Poincaré [18] to describe the long-time-behaviour of the motion of the planets in the solar system. The dynamics of the planets can be described in a good approximation by a fast rotation around the sun on elliptic orbits, where the eccentricity and the point of culmination change comparatively slowly but with a complex dynamic. Is the motion of the point of culmination chaotic, periodically oscillating, stable or unstable, the whole dynamics generically possess this property. In this way the dynamics of the solar system [19] and the dynamics of a huge variety of other systems [11–13, 20], composed of smooth oscillations with a time varying amplitude or phase, can be well described with Poincaré-maps. Also the stroboscopic map $\underline{g}(\underline{x}, T)$, which maps the state vector $\underline{x}(t)$ at the time t into the state vector at the time $t + T$, $\underline{g}(\underline{x}(t), T) = \underline{x}(t + T)$, can give a simple description of the long-time behaviour, especially for systems with periodic drive, if $T \gg 0$ is well chosen (for example synchronously to the driving force). In Figs. 1 and 2 the stroboscopic maps of a Van-der-Pol-

* Part of Ph.D. thesis

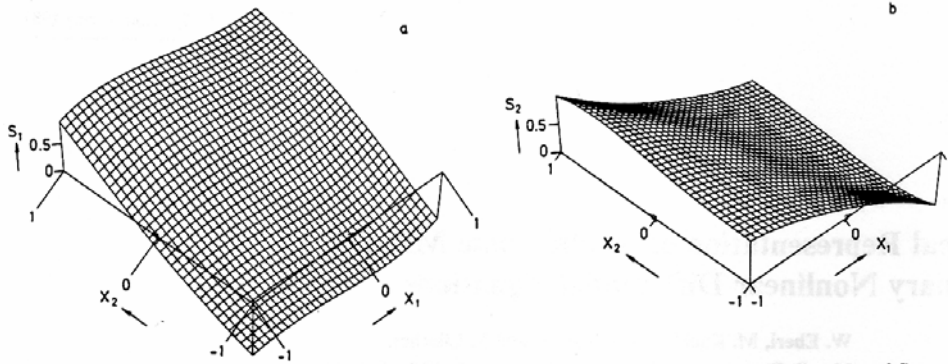


Fig. 1. The first and second component of the stroboscopic map $\mathcal{g}_n(x, 1.6)$ of a Van-der-Pol oscillator (Eq. 1, $\epsilon=0.5$) versus the initial conditions x

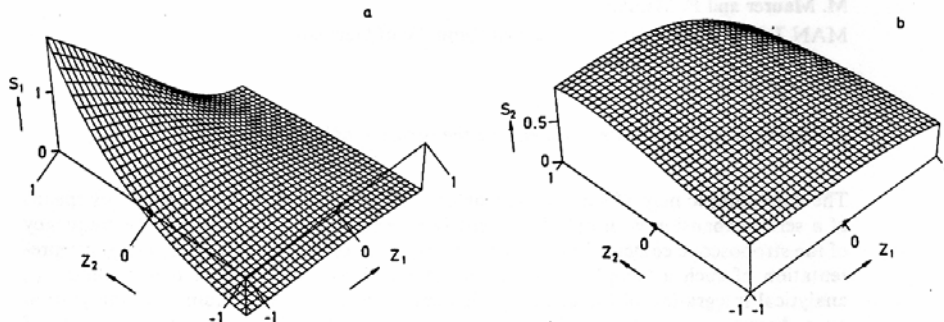


Fig. 2. The first and second component of the stroboscopic map $\mathcal{g}_n(x, T_0 = \frac{2\pi}{\omega})$ of the x^3 -oscillator (Eq. 2, $g=0.97$) versus $z_1 = 0.8(x_1 + x_2) + 0.15$ and $z_2 = 0.8(x_1 - x_2) + 0.15$ with $x_3 = 0$. The index n indicates that the map is calculated numerically (by a Runge-Kutta-algorithm of 5th-6th order)

oscillator:

$$\begin{aligned} \dot{x}_1 &= x_2 \\ \dot{x}_2 &= e(0.25 - 2x_1^2)x_2 - x_1, \quad e > 0 \end{aligned} \tag{1}$$

and of a damped oscillation in a cubic potential, driven by a sinusoidal force (x^3 -oscillator, or Helmholtz oscillator):

$$\begin{aligned} \dot{x}_1 &= x_2 \\ \dot{x}_2 &= -g x_2 - 0.65 x_1 + x_1^2 - 0.36667 - 0.835 \cos \omega x_3 \\ \dot{x}_3 &= 1, \quad \omega = 0.806, \quad g > 0 \end{aligned} \tag{2}$$

are shown. Although the differential equation of the x^3 -oscillator possesses only a quadratic nonlinearity, its dynamics and its route to chaos is closely related [20] to that of a Duffing-Oscillator [2, 3] and to that of driven, damped oscillations in a Todapotentia [2].

In the following it will be illustrated that even chaotic dynamics, generated from a nonlinear differential equation, can be well approximated by simple maps, which can be described by means of a series expansion with only few non-trivial coefficients. Two methods to derive an analytic expression for stroboscopic maps and Poincare maps will be presented: (i) the numerical integration on a special grid scheme, and (ii) analytical integration.

2. Analytic Representation of Iteration Maps by Numeric Integration on a Special Grid Scheme and a Fit

An analytic expression of stroboscopic maps and Poincare-maps of a n -dimensional nonlinear autonomous differential equation

Table 1. Coefficients a_{ik}^j of $\underline{s}_n(z, T_0) = \begin{pmatrix} s_1 \\ s_2 \\ s_3 \end{pmatrix}$ of the x^3 -oscillator for

$g = 0.97, z_3 = 0$ with $s_j = \sum_{i,k=0}^3 a_{ik}^j z_1^i z_2^k, j = 1, 2, 3, s_3 = T_0 + z_3$ calculated by Tschebyscheff approximation of third order. At 121 grid points the differential equation was integrated numerically [22]

i	k	a_{ik}^1	a_{ik}^2	i	k	a_{ik}^1	a_{ik}^2
0	0	-0.333	1.043	2	0	-0.166	-0.200
0	1	0.488	0.231	2	1	-0.014	-0.108
0	2	0.086	-0.052	2	2	0.261	-0.055
0	3	-0.035	-0.022	2	3	0.184	-0.046
1	0	-0.425	-0.201	3	0	0.611	-0.088
1	1	-0.728	-0.182	3	1	0.210	-0.032
1	2	-0.464	-0.006	3	2	0.097	0.008
1	3	-0.108	0.028	3	3	-0.028	0.026

Table 2. The maximal deviation Δs of the map calculated by a Runge-Kutta-method $\underline{s}_n(x, 1.6)$ from the map $\underline{s}_n(x, 1.6)$ for several Van-der-Pol oscillators (Eq. 1)

e	p	s	e	p	s
0.01	3	$5 \cdot 10^{-6}$	0.5	10	$5 \cdot 10^{-6}$
0.2	3	$4 \cdot 10^{-3}$	3.0	5	$1 \cdot 10^{-1}$
0.5	3	$2 \cdot 10^{-2}$	3.0	10	$2 \cdot 10^{-2}$
0.5	5	$1.6 \cdot 10^{-3}$	3.0	15	$4 \cdot 10^{-3}$

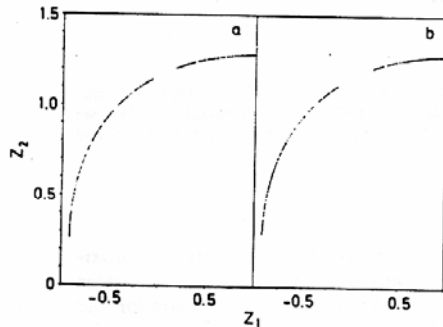


Fig. 3a and b. Poincaré-section generated numerically by a Runge-Kutta algorithm (a) and by $\underline{s}_n(z, T_0)$ with $p = 5$ and $g = 0.97, z_3 = 0$ (b)

$$\dot{x} = f(x) \tag{3}$$

$\left(x = \begin{pmatrix} x_1 \\ \vdots \\ x_n \end{pmatrix} \right)$ = state vector, $f = n$ -dimensional flow vector

field) are investigated in three steps:

- the state vector x is transformed to a state vector

$z = \begin{pmatrix} z_1 \\ \vdots \\ z_n \end{pmatrix}$ = such, that the region of interest, e.g. the

surroundings of an attractor are covered by the region $(z | -1 < z_1 < 1 \dots -1 < z_n < 1)$. The size of an attractor can be numerically estimated.

- the map is numerically calculated for those initial conditions z which correspond to the Tschebyscheff-abscisses [22].

- with the help of the Tschebyscheff-polynoms a polynomial approximation of degree p in each variable of the map is calculated.

If the variables of the x^3 -oscillator (Eq. (2)) are transformed in the following way $z_1 = 0.15 + 0.8 x_1 + 0.8 x_2, z_2 = 0.15 + 0.8 x_1 - 0.8 x_2, z_3 = x_3$ the stroboscopic map $\underline{s}_n(z, T)$ in the domain $(z | -1 < z_1 < 1,$

$-1 < z_2 < 1, 0 < z_3 < T_0, 0 < T < T_0 = 2 \frac{\pi}{\omega})$ can be ap-

proximated by a cubic map $\underline{s}_n(z, T_0)$ (Table 1). This domain nearly coincides with that part of the state space which is filled more or less densely by the attractor. The maximal deviation of the approximation \underline{s}_n from the numerically investigated map \underline{s}_n is small in this area, e.g. $\Delta s = \max |\underline{s}_n(z, T_0) - \underline{s}_n(z, T)| / s < 4 \cdot 10^{-2}$, with $z_3 = 0, p = 3$ and

$$s = \int_{-1}^1 \int_{-1}^1 dz_1 dz_2 \cdot |\underline{s}_n(z_1, z_2, z_3 = 0, T_0)| / \int_{-1}^1 \int_{-1}^1 dz_1 dz_2.$$

For $p = 5$ results $\Delta s < 1.5 \cdot 10^{-3}$ for $z_3 = 0$. The chaotic dynamics investigated with these maps \underline{s}_n corresponds well with the numerically investigated dynamics [22], as the appropriate Poincaré-section (Fig. 3) shows. The numeric integration by a Runge-Kutta-method of fifth order needs 6 CPU-s (Cyber 975) to calculate the Poincaré-section (1000 oscillations), whereas for the approximation of the stroboscopic map by a map of fifth order 0.38 CPU-s and for the following 1000 iterations 0.5 CPU-s were needed.

In the same way the stroboscopic map of a Van-der-Pol-Oscillator (Eq. (1)) can be investigated. The maximal deviation $\Delta s = \max |\underline{s}_n(x, 1.6) - \underline{s}_n(x, 1.6)| / s$ with

$$s = \int_{-1}^1 \int_{-1}^1 dz_1 dz_2 |\underline{s}_n(x_1, x_2, 1.6)| / \int_{-1}^1 \int_{-1}^1 dx_1 dx_2$$

depends on the order p of the approximation and the asymmetry parameter e of the Van-der-Pol oscillator (Table 2).

3. Analytic Representation of the Stroboscopic Map by Analytic Integration

The stroboscopic map is investigated by integration of the ordinary differential equation over the certain time span $T \gg 0$. The integration by means of a Euler's method [23] or a Runge-Kutta-Algorithm can be done analytically by means of algebra-manipulation-programs. If for example Euler's method is used the time span T is separated in m parts and m iterations are carried out:

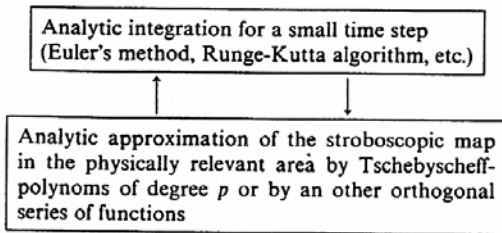
$$x(i dt + dt + t) = x(i dt + t) + dt f(x(i dt + t)) \quad (4)$$

whereby $dt = T/m$, $i = 0 \dots m-1$, $x_0 = x(t)$ = initial condition at time t , f = flow vector field (Eq. (3)). The stroboscopic map $\underline{x}_m(x_0, T)$ is obtained from the iteration:

$$\underline{x}_m(x_0, (i+1) dt) = \underline{x}_m(x_0, i dt) + dt f(\underline{x}_m(x_0, i dt)) \quad (5)$$

with the initial condition: $\underline{x}_m(x_0, 0) = x_0$. If the components of f can be represented as polynomials in the components of x_0 , then, due to the initial condition, for the components of $\underline{x}_m(x_0, i dt)$ polynomials of degree r result. The degree r grows with every iteration step, if the degree of the polynomial of a component of f is greater than 1, i.e. the ordinary differential equation, is nonlinear. Numeric integration and approximation of the stroboscopic map of the x^3 -oscillation as presented in Chap. 3 shows however, that in this system the physically relevant area of the stroboscopic map can be successfully approximated by the cubic map in the time interval $[0, \frac{2\pi}{\omega}]$. Therefore we propose

the following procedure for the analytic integration:



If one uses such an analytic integration for a Van-der-Pol-Oscillator (1) with asymmetry parameter $e=0.5$, the analytically calculated iteration function (Table 3) approximates already for $p=3$ the trajectories calculated with a Runge-Kutta-algorithm very well (Fig. 4). The differences between the trajectories calculated nu-

Table 3. Coefficients a_{ik}^j of $\underline{x}_m(x, 1.6) = \begin{pmatrix} s_1 \\ s_2 \end{pmatrix}$, with $s_j = \sum_{i,k=0}^3 a_{ik}^j x_1^i x_2^k$ and $j=1, 2$ of the Van-der-Pol oscillator (Eq. 1, $e=0.5$) calculated by analytic integration.

i	k	a_{ik}^1	a_{ik}^2	i	k	a_{ik}^1	a_{ik}^2
0	1	1.117	0.003	2	1	-0.227	0.253
0	3	-0.176	-0.179	2	3	0.130	0.005
1	0	-0.105	-1.147	3	0	-0.260	0.241
1	2	-0.150	0.354	3	2	0	-0.266

All the other coefficients are zero. The deviation of these coefficients from those calculated by a numeric integration and a fit with Tschebyscheff polynomials ($p=3$) is smaller than $2 \cdot 10^{-2}$, the maximum deviation of the corresponding map $\underline{x}_m(x, 1.6)$ from $\underline{x}_m(x, 1.6)$ $\Delta s < 2 \cdot 10^{-2}$

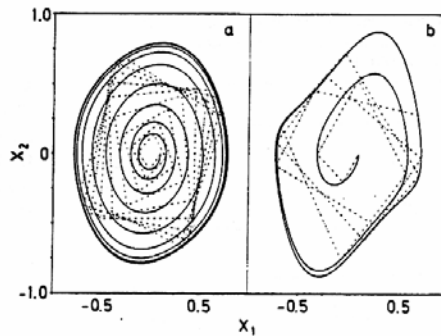


Fig. 4a and b. Trajectories of a Van-der-Pol oscillator (— = integration by a Runge-Kutta method, - - - = straight line between the states generated by $\underline{x}_m(x, 0.25)$) with $p=3$ for $e=0.5$ (a) and $p=10$ for $e=3$ (b)

merically and those calculated by an analytic approximation are essentially smaller than those of former investigations [24, 25]. The route to chaos for the x^3 -oscillator can be reproduced with the analytically investigated stroboscopic map. In Fig. 5 the z_1 -values of a Poincare-section of the x^3 -oscillator are represented as function of the friction coefficient g . All three methods show good agreement. The analytic integration and the analytic approximation were formulated as tensor operations which act on the coefficient tensors and were implemented in Fortran. The analytic integration for polynoms up to 5th degree need at 200 integration steps about 100 CPU-s (Cyber 975). An implementation in the algebra manipulation language REDUCE [26] needs for the same task 5th CPU-time on a VAX 780 (9 MByte), mainly due to problems with the limited heap space and the arithmetic of small real numbers.

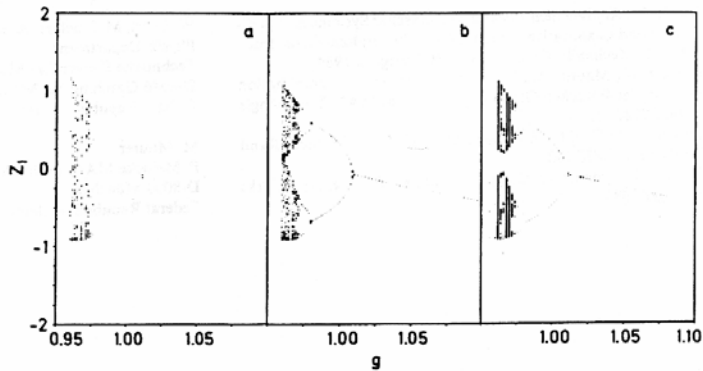


Fig. 5a-c. Bifurcation diagram of the variable z_1 versus the friction coefficient g of the x^3 -oscillator (Eq. 2) generated by $\underline{s}(z, T_0)$ with $p=5, z_3=0$ (a), $\underline{s}_h(z, T_0)$ with $p=5, z_3=0$ (b) and $\underline{s}_h(z, T_0)$ (c) with $z_3=0$

4. Outlook

The stroboscopic maps were separately investigated for all friction coefficients g . If one expands the stroboscopic map with respect to the parameters of the differential equation, it should be possible to consider the dependence of the stroboscopic map on the parameters of the differential equation analytically. Problems arise because the order of the coefficient tensors of the relevant series expansion grows linearly with the number of parameter and therefore the order of the corresponding transformation tensors become very large in the analytic procedure. In the approximative numerical approach (Chap. 2), the minimum number of the grid points necessary for a fit increases strongly.

As the typical dynamics of the stroboscopic map $d/dT \underline{s}(x_0, T) = \underline{f}(\underline{s}(x_0, T))$ is ruled [27] by a few unstable modes, it may be possible to describe the dynamics of the coefficients by a low-dimensional ordinary differential equation system. This system has to be solved for the set of initial conditions for the modes amplitudes (for example numerically), which follows from the condition $\underline{s}(x_0, 0) = x_0$. The differential equation for the amplitudes of the modes can be investigated again analytically in the physically relevant area, namely the value area of the amplitudes of the modes, which arises from the specific initial condition.

We like to thank H. Haken, W. Kroy, O. Wohofsky, P. Deisz, A. Hayd, W. Satzger and Ch. Berding for their continuous support. This work was supported in part by MBB.

References

1. Lichtenberg, A.J., Lieberman, M.A.: Regular and stochastic motion. Chap. 5.5. Berlin, Heidelberg, New York: Springer 1982

2. Lauterborn, W., Cramer, E.: Phys. Rev. Lett. 47, 1445 (1981); Parlitz, U., Lauterborn, W.: Phys. Lett. 107A, 351 (1985); Klinker, T., Meyer-Ilse, W., Lauterborn, W.: Phys. Lett. 101A, 371 (1984)
3. Huberman, A., Crutchfield, J.P.: Phys. Rev. Lett. 43, 1743 (1979); Crutchfield, J.P., Huberman, B.A.: Phys. Lett. 77A, 407 (1980); Humieres, D.D., Beasley, M.R., Huberman, B.A., Libchaber, A.: Phys. Rev. A 26, 3483 (1982)
4. Babloyantz, A., Salazar, J.M., Nicolis, C.: Phys. Lett. 111A, 152 (1985)
5. Weitz, D.A., Huang, J.S., Lin, M.Y., Sung, J.: Phys. Rev. Lett. 54, 1416 (1985)
6. Guckenheimer, J., Buzyna, G.: Phys. Rev. Lett. 51, 1438 (1983)
7. Haken, H.: Synergetics. Chap. 8. Berlin, Heidelberg, New York: Springer 1983
8. Ruelle, D., Takens, F.: Commun. Math. Phys. 20, 167 (1971)
9. Schuster, H.: Deterministic chaos. p. 175. Weinheim: Physik-Verlag 1984
10. Eilenberger, G.: In: Nichtlineare Dynamik in kondensierter Materie; Eilenberger, G., Müller-Krumbhaar, H. (eds.), Kernforschungsanlage-Jülich, D-Jülich, 1985
11. Swinney, H.L.: Physica 7D, 3-15 (1983)
12. Lorenz, E.N.: J. Atmos. Sci. 20, 130 (1963)
13. Lichtenberg, A.J., Lieberman, M.A.: Regular and stochastic motion. p. 28, pp. 95ff. Berlin, Heidelberg, New York: Springer 1982
14. Collet, P., Eckmann, J.P.: Iterated maps of the interval as dynamical systems. Boston: Birkhäuser 1980
15. Feigenbaum, M.: J. Stat. Phys. 19, 25 (1978)
16. Mandelbrot, B.B.: Physica 7D, 224 (1983)
17. Richter P.: The beauty of fractals: images of complex dynamical systems. Berlin, Heidelberg, New York: Springer 1986
18. Poincare, H.: Les Methodes Nouvelles de la Mechanique Celeste. Paris: Gautier-Villars 1892
19. Richter, P.: Preprint 1987
20. Wachinger, C., Hübler, A., Reiser, G., Lüscher, E.: Helv. Phys. Acta 59, 132 (1986)
21. Bjoerck, A., Dahlquist, G.: Numerische Methoden. p. 91. München: Oldenbourg 1979
22. Program DVERK of the IMSL library (IMSL, 7500 Bellaire Boulevard, Houston, Texas, USA) a Ruge-Kutta-algorithm of 5.-6. order
23. Bjoerck, A., Dahlquist, G.: Numerische Methoden. p. 7. München: Oldenbourg 1979

24. Bestle, D.: Analyse nichtlinearer dynamischer Systeme mit qualitativen und quantitativen Methoden. p. 59. Diplom-thesis, Institut B für Mechanik of the Universität Stuttgart, 1984
 25. Satzger, W., Maurer, M., Hayd, A.: Analytische Approximation der Van-der-Pol'schen Gleichung. München: MAN-Technologie Publ. B99801 1985
 26. Hearn, A.C.: REDUCE – Users Manual. Santa Monica: Rand Publication CP78 1983
 27. Haken, H.: Synergetics. Chap. 7. Berlin, Heidelberg, New York: Springer 1983
- W. Eberl, M. Kuchler, A. Hübler, E. Lüscher
Physik-Department
Technische Universität München
D-8046 Garching bei München
Federal Republic of Germany
- M. Maurer
P. Meincke MAN Technologie
D-8000 München
Federal Republic of Germany